Review

Amphiphilic polysilane-methacrylate block copolymers
— Formation and interesting properties —

By Hideki Sakurai[*),†)]

Professor Emeritus, Tohoku University

(Communicated by Teruaki Mukaiyama, m.j.a.)

Abstract: Several polysilane block copolymers have been prepared by the newly developed method, anionic polymerization of masked disilenes. Especially amphiphilic block copolymers of poly(1,1-dimethyl-2,2-dihexyldisilene) and poly methacrylate are focused. Poly(1,1-dimethyl-2,2-dihexyldisilene)-b-poly(2-hydroxyethyl methacrylate) (PMHS-b-PHEMA) is the first example of the amphiphilic polysilane copolymer that can form micelles in polar solvents. Poly(1,1-dimethyl-2,2-dihexyldisilene)-b-poly(methacrylic acid) (PMHS-b-PMAA) is more polar than (PMHS-b-PHEMA), soluble in water to form micelles. The cross-linking reaction of (PMHS-b-PMAA) with 1,10-diaza-4,7-dioxadecane and 1-ethyl-3-(3-dimethylaminopropyl)carbodiimide hydrochloride afforded the first shell cross-linked micelles (SCM) of polysilane. In addition to interesting properties, SCM is indicated to be able to form hollow sphere particles (hollow shell cross-linked micelles, HSCM) by a photochemical process. Reversible encapsulation of guest molecules by SCM and HSCM is demonstrated. Finally, SCM can be used as the template for the synthesis of metal nanoparticles, which may be used as catalysts.

Key words: Polysilane; amphiphilic block copolymer; shell-crossed micelle (SCM); hollow-sphere shell-crossed micelle (HSCM); encapsulation; metal nanoparticles.

Introduction. Polysilanes,[1)] Si-Si σ-bonded polymers, are structurally analogous to C-C σ-bonded polymers such as polyethylene and polystyrene because they have linear homocatenated backbones. They are relatively thermally stable with proper substituents. However, due to high orbital energies (or low ionization energies) of Si-Si σ-orbitals and σ-conjugation, polysilanes exhibit several interesting electronic and optical properties, which often characterize polysilanes as one-dimensional electronic wires. Thus during the last decades, polysilanes have been widely investigated because of their potential applications in the field of materials science (Fig. 1).

Polysilanes are usually prepared by the Wurtz-type reductive coupling of dichlorosilanes with alkali metals (Fig. 2). Although many kinds of polysilanes have been prepared by this method, the structure of the polymers is difficult to control. Molecular weight and polydispersity are also unmanageable. These are weak points, which must be overcome for further development of polysilane chemistry. Several other methods, such as dehydrogenative coupling and ring-opening polymerization have been reported but none of them are satisfactory for controlling the structure (Fig. 2).

In regard to this point, we have developed a novel method of polysilane synthesis based on anionic polymerization of masked disilenes (i.e. 1-phenyl-7, 8-disilabicyclo[2.2.2]octa-2,5-diene derivatives, **1**) to obtain polysilanes with highly controlled structures since 1989.[2)] In fact, at this moment, this is the sole method of obtaining polysilanes with highly controlled structure (Fig. 3).

For example, poly(1,1-dimethyl-2,2-dihexyldisilene) (PMHS, **3**), obtained by this method, shows

Fig. 1.   Characteristics of polysilanes.

Fig. 2.   Conventional preparation of polysilanes.

Fig. 3.   Anionic polymerization of masked disilenes.

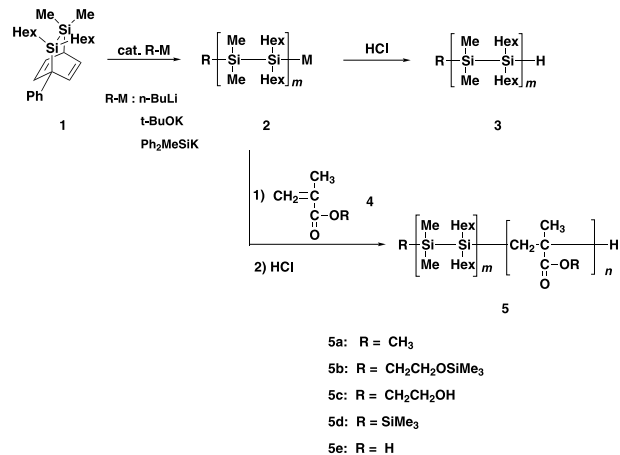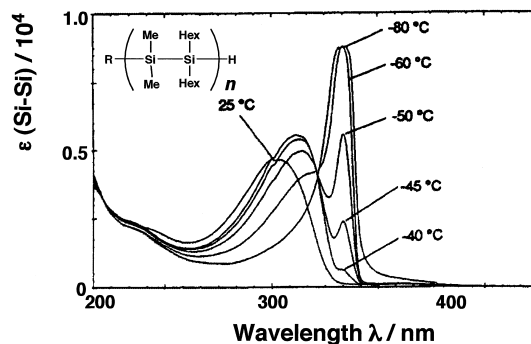Fig. 4.   Temperature dependent UV spectra of poly(1,1-dimethyl-2,2-dihexyldisilene) (**3**) due to conformational change.

highly ordered structure[3] and as a result, unique abrupt thermochromism both in solution and in the solid state (Fig. 4).[4] Origin of the thermochromism is attributed, at least in part, to abrupt conformational transition from trans (or transoid) to cis (or cisoid) structures. The polysilane takes the former conformation in solution at high temperature, while the latter in solution at low temperature or in solid.

One of the profitable aspects of the method involves living anions (**2**) in the polymerization, which can be used for block copolymerization with a second monomer such as methacrylate (**4**).[2,5] The block copolymers (**5**) can be prepared also with highly controlled structure. Combinations of interesting electronic properties of polysilanes and mechanical as well as chemical properties of methacrylates provide useful possibilities in applications for the block copolymers. In this review, the author will describe recent progress concerning the polysilane block copolymers.

Amphiphilic block copolymers of polysilane with methyl methacrylate. The first copolymers of polysilane dealing with in this review are poly(1,1-dimethyl-2,2-dihexyldisilene)-*b*-

Table I.   Solubility of **5a** and other related polymers

solvent	**5a**	PMHS	PMMA
hexane	+	+	−
toluene	+	+	+
acetone	+	−	+
ethanol	−	−	−

+: Soluble more than 2×10^{-2} g.l^{-1}. −: Insoluble.

poly(methyl methacrylate) (PMHS-*b*-PMMA, **5a**, R = CH$_3$), which can be prepared by the copolymerization with a conventional monomer, methyl methacrylate as illustrated in Fig. 3.[2] Subsequent studies indicate the possibility of the formation of micelles for the copolymer.[6] As shown in Table I, the copolymers **5a** are soluble in both non-polar hexane and polar acetone, indicating an amphiphilic property. The formation of particles in toluene/methanol mixed solvent is demonstrated as well, but the PMMA block copolymer is insoluble in ethanol and hence is not polar enough for further studies on aggregates.

Amphiphilic block copolymers of polysilane with 2-hydroxyethyl methacrylate. The formation of polysilane micelles. To increase the polarity of the block copolymers, we have studied next poly(1,1-dimethyl-2,2-dihexyldisilene)-*b*-poly(2-hydroxyethyl methacrylate) (PMHS-*b*-PHEMA, **5c** R = CH$_2$CH$_2$OH). Poly(1,1-dimethyl-2,2-dihexyldisilene) (PMHS) was selected again as the polysilane block, since this polysilane shows abrupt thermochromism in solution and also in the solid state as described before. For the polar block, we have adopted poly(2-hydroxyethyl methacrylate) (PHEMA). PHEMA was introduced first by Nakahama *et al.* as a typical hydrophilic polymer.[7] We have expected that the amphiphilic copolymer would be soluble in polar solvents to form micelles, where hydrophobic polysilanes exist in the form of core inside a hydrophilic corona (enclosure). It is interesting to examine the electronic properties of polysilanes existing in the core of micelles.

Two samples of block copolymers, with different relative lengths of their blocks, were prepared by the anionic polymerization of the masked disilene **1**, followed by the second polymerization with 2-(trimethylsilyloxy) ethyl methacrylate (**4b**, R = CH$_2$CH$_2$OSiMe$_3$). Hydrolysis of the trimethylsilyl protecting groups of the resulting diblock copolymer (**5b**, R = CH$_2$CH$_2$OSiMe$_3$) gave the desired block copolymers, PMHS-*b*-PHEMA (**5c**, R =
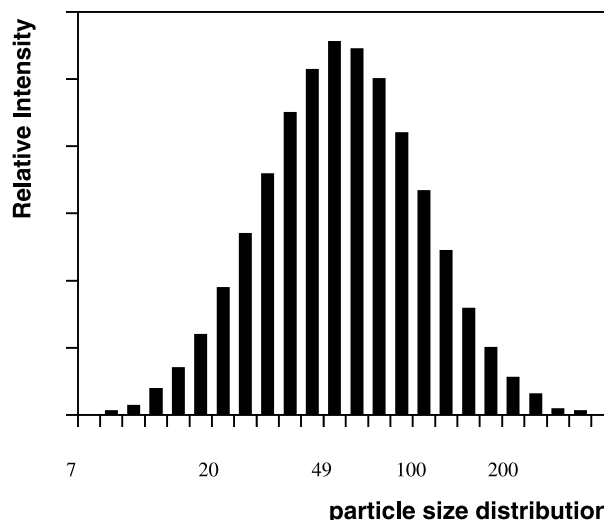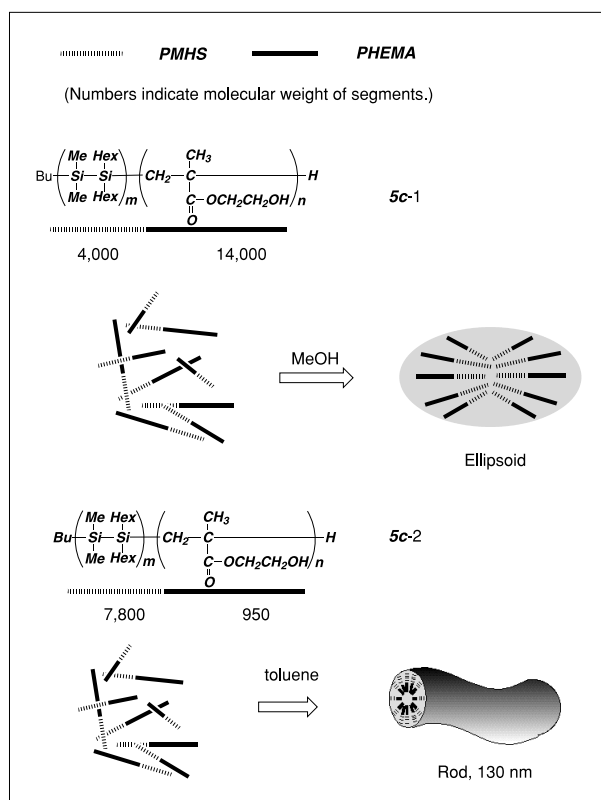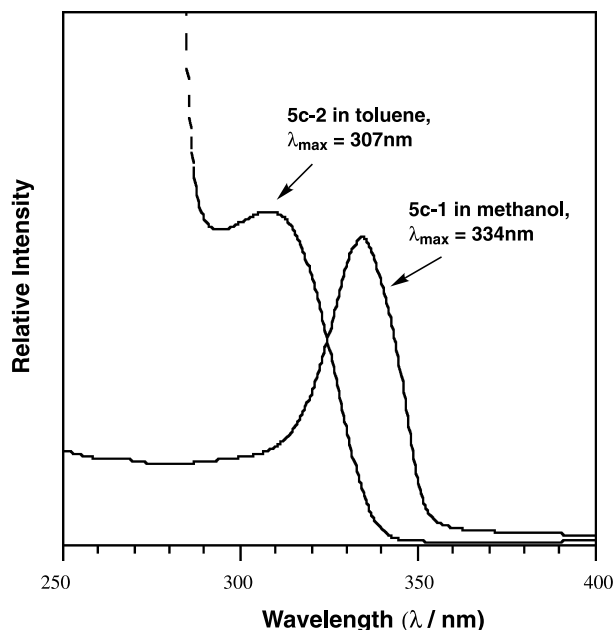

Fig. 5.   Particle size distribution of **5c**-1 determined by DLS.
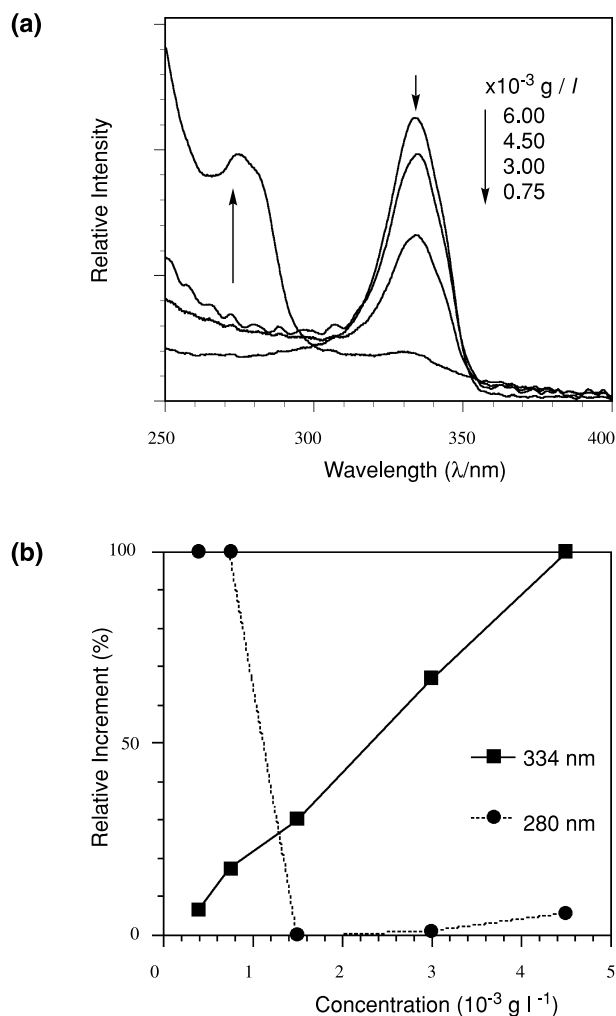

Fig. 6.   Formation of aggregates.

CH$_2$CH$_2$OH).[8]

The copolymer with a longer PHEMA (**5c**-1) was insoluble in both hexane and toluene but appar-

Fig. 7.   UV Spectra of **5c**-1 and **5c**-2.

Fig. 8.   (a) Concentration dependent UV spectra of **5c**-1 in methanol (determination of CMC) and (b) relative intensities at 334 and 280 nm.

ently soluble in methanol. It was thought to form a colloidal solution. In fact, dynamic light scattering (DLS) experiments in methanol (0.046 g/l, 20 °C) indicated a monodispersed particle size distribution (Fig. 5), the Z-averaged particle size being estimated as 50 nm. Since the calculated molecular length of the polymer is *ca.* 20 nm, the copolymer should form sphere-like aggregates (micelles). Indeed, static light scattering (SLS) experiments demonstrated the shape of the copolymer to be ellipsoidal (Fig. 6). The copolymer with longer PMHS chains (**5c**-2) dissolves in toluene, but also forms aggregates. In contrast to **5c**-1, light scattering studies indicate that **5c**-2 should form aggregates with an average size of 150 nm having a rod like anisotropic shape at the polymer concentration of 0.046 g/l under the conditions (Fig. 6).

Fig. 7 shows the UV spectra of these two copolymers, where **5c**-1 in methanol exhibits λ_{max} at 334 nm while **5c**-2 in toluene shows λ_{max} at 307 nm. The absorption at 334 nm of **5c**-1 is identical to the absorption of PMHS in the solid state at room temperature, where the PMHS block takes a trans conformation. These spectroscopic characteristics indicate that in **5c**-1, the PMHS block exists in the hydrophobic core as a solid surrounded by the hydrophilic PHEMA block, while in **5c**-2, the PMHS block exists in a corona being exposed to toluene,

a good solvent for PMHS, where the PMHS block takes a random conformation.

It is interesting to examine whether these amphiphilic block copolymers show critical micellization phenomena because it is a fundamental process in colloid formation.[9] Fig. 8 shows the dependence of UV absorption of **5c**-1 on concentrations. Absorption at 334 nm due to all-trans solid states decreased upon dilution from 6.00×10^{-3} g/l and disappeared almost completely at 0.75×10^{-3} g/l with evolution of a new absorption at 280 nm due to the random coil structure. These spectral characteristics could be reasonably explained by synchronized conformational changes of the PMHS block with micelle formation. The micelle structures of **5c**-1, with a

PMHS block in the core, are maintained at concentrations down to 0.75×10^{-3} g/l and then micelles are destroyed upon further dilution to give a unimer in solution, which adopts random coil structures. This particular concentration should correspond to the critical micelle concentration (CMC) under the conditions. **5c**-1 is a class of kinetically frozen micelles above the CMC at low concentration, since no absorption due to the random coil structure, which should exist in solution if exchange occurred, was observed above the CMC.[10]

Next, the dynamic behavior of the copolymer **5c**-1 on changing the solvent composition was studied. The absorption maximum of **5c**-1 at 334 nm in 100% methanol (0.02 g/l) decreased on addition of toluene while keeping the concentration of the copolymer constant (Fig. 9). A new peak at around 310 nm started to grow as a shoulder (methanol/toluene = 70/30) when toluene was added and then the peak grew constantly. Interestingly, DLS experiments indicated that the average particle size of 80 nm in 100% methanol decreased to 20 nm in a methanol/toluene (70/30) mixed solvent. Then the particle size increased again to 140 nm on increasing the toluene proportion further (methanol/toluene = 40/60). Since a particle size of 20 nm corresponds to that of the unimer, the observed phenomena could be explained as follows: the micelles with PMHS in the core are destroyed by adding toluene and then form another aggregate with PMHS as corona (reverse micelle).

Since **5c**-1 forms kinetically frozen micelles and the component polysilane block has a glass transition temperature (T_g) higher than room temperature, it is expected that the morphology of the copolymer can be observed directly by the technique of atomic force microscopy (AFM) operating in the tapping mode.[11] Structures of the copolymer **5c**-1 in the solid film on mica coated from a methanol solution (0.043 g/l) indicated ellipsoidal structures with a size of 50-60 nm in agreement with SLS experiments.

Encapsulation of polysilane into shell cross-linked micelles. The formation and properties of shell cross-linked micelles (SCM) have been investigated actively in recent years because of the possibility of construction of stable particles.[12] The macromolecular architectures of SCM are nanometer-sized, with amphiphilic core-shell spheres that are prepared by the self-assembly of amphiphilic block copolymers into polymer micelles, followed by
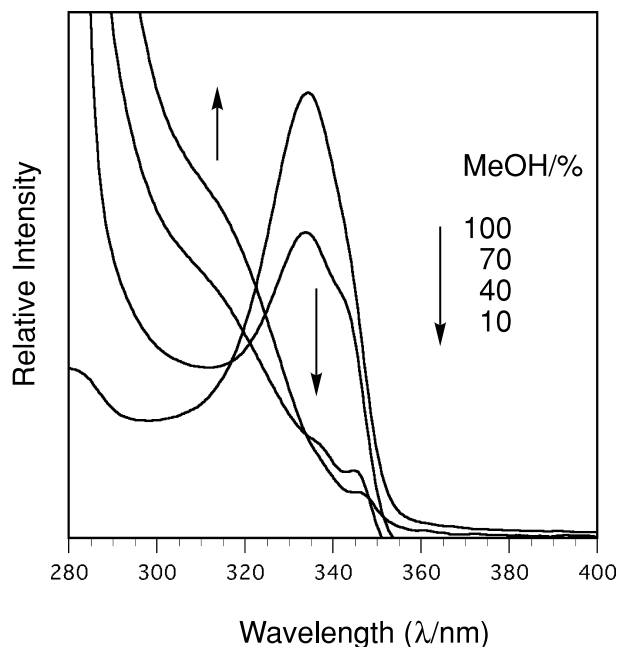

Fig. 9. UV Spectral change of **5c**-1 on solvent composition in toluene-methanol (solvato-chromism).

cross-linking of the side chains along the block composing the shell of the polymer micelles. It should be interesting to prepare SCM with polysilanes in the core and to investigate the behavior.

Accordingly, we have prepared poly(1,1-dimethyl-2,2-dihexyldisilene)-*b*-poly(methacrylic acid) (PMHS-*b*-PMAA, **5e**, R = H) by the sequential anionic polymerization of **1** and trimethylsilyl methacrylate (**4e**, R = SiMe$_3$), followed by hydrolysis of the trimethylsilyl protecting group.[13]

Since the copolymer **5e** is insoluble in chloroform, it was necessary to convert **5e** to soluble methyl ester by the reaction with diazomethane for molecular weight determination. Then the molecular weight was estimated by size exclusion chromatography (SEC) with CHCl$_3$ as an eluent (Mn = 2.8×10^4, Mw/Mn = 1.07, calibrated with polystyrene standards). The molecular weight of **5e** was then estimated to be Mn = 2.4×10^4. PMHS-*b*-PMAA (**5e**), which is soluble in water, is expected to self-assemble in water to form polymer aggregates. In fact, dynamic light scattering (DLS) studies indicated the formation of near-monodisperse micelle, with an intensity-averaged micelle diameter of 170 nm in water (0.2 g/l, 25 °C). Since the calculated length of the stretched copolymer is about 60 nm with an assumption of all trans conformation, the micelle may

Fig. 10.   Schematic illustration of synthesis of organized systems.

Fig. 11.   Preparation of SCM-5e by sequential reactions.

Fig. 12.   AFM Images of shell cross-linked micelles (SCM-5e).

be swollen to some extent.

Since **5e** has a reactive methacrylic acid block, the shell cross-linking reaction of the polymer micelles was examined by a scheme outlined in Fig. 10. A solution of the polymer micelles was prepared in water at a concentration high enough to allow the formation of micelles. The shell cross-linking of the carboxylic acid on the poly(methacrylic acid) block of **5e** was achieved by the reaction with 1,10-diaza-4,7-dioxadecane and 1-ethyl-3-(3-dimethylaminopropyl) carbodiimide hydrochloride to the solution (Fig. 11). After the cross-linking reaction, ^{1}H NMR signals of the cross-linked block copolymer could not be detected in D_2O solution because of very long relaxation times due to its colloidal nature, despite the apparent solubility. Although an equivalent amount of cross-linking reagent to the methacrylic acid units was used, the proportion of the cross-linked methacrylic acid units on the block copolymer to the uncross-linked was *ca.* 50%

as estimated by ^{1}H NMR in D_2O-THF-d_8.

In the solid state CP-MAS ^{29}Si NMR of SCM-**5e**, two signals were observed at -27.6 and -35.7 ppm, assignable to dihexylsilylene and dimethylsilylene units, respectively. The IR spectrum of SCM-**5e** shows absorption bands for both the carboxylic acid and the amide groups at 1710, 1631, and 1569 cm^{-1}, although that of **5e** shows only the absorption band for the carboxylic acid at 1702 cm^{-1}. The DLS studies indicated the intensity-averaged diameter of the particles to be 160 nm with mono-dispersed spheres, which agreed very closely with the size of the original micelles composed of the block copolymer **5e** (170 nm). Interestingly, DLS studies indicated that SCM-**5e** in THF was mono-dispersed, the intensity-averaged diameter of the particles being 230 nm. Since the (uncross-linked) block copolymer **5e** in THF does not form particles, the formation of the SCM from **5e** is indicated clearly. Significant change in particle sizes was observed, which must result from the solvated PMHS blocks under the conditions.

An atomic force microscopy (AFM) image of SCM-**5e** provided information on the size and shape of the shell cross-linked spheres. Fig. 12 shows the AFM image of SCM-**5e** film on a Pyrex glass plate operating in the contact mode. Spherical particles of *ca.* 25 nm diameter in the dry state are clearly observed. Under the conditions, the cross-linked corona will eventually shrink onto the glassy PMHS core as
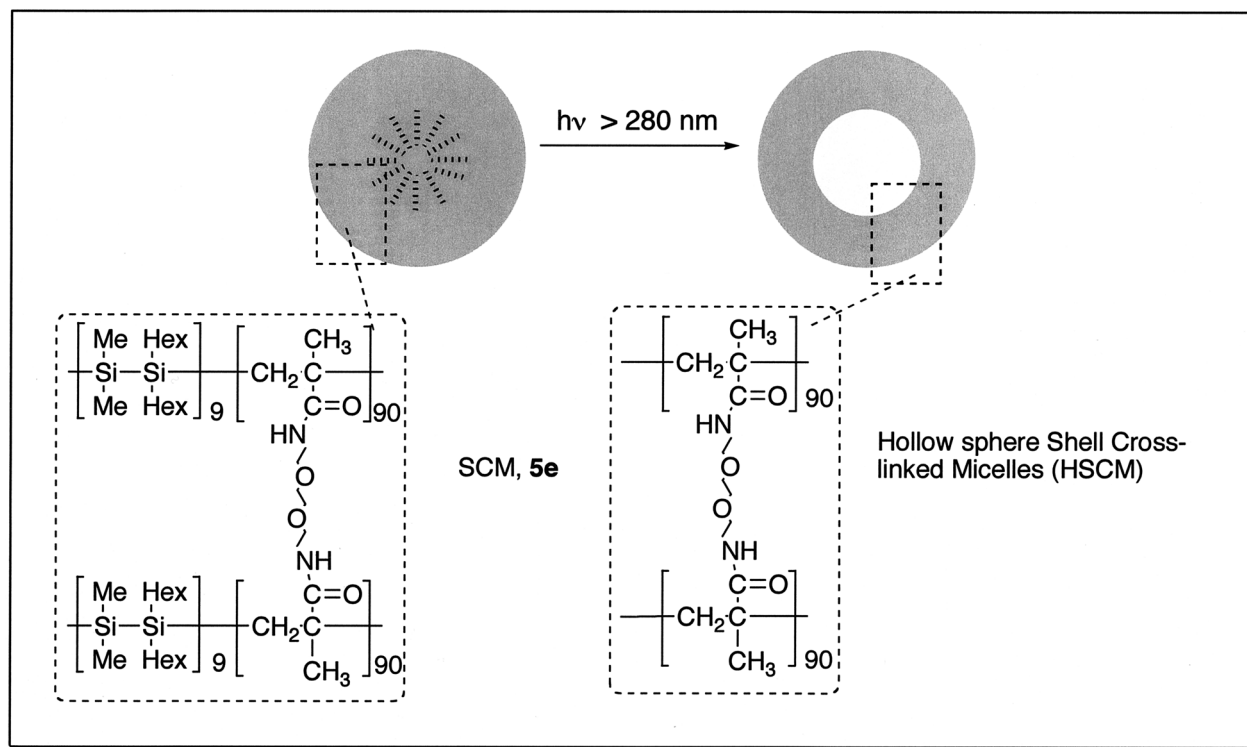
Fig. 13.   The preparation of nanometer-sized hollow particles by photochemical degradation of polysilane shell cross-linked micelles.

the film dries. The measured radius of the dry sphere may fit the molecular length of **5e**.

It is worthwhile to examine the electronic properties of the polysilanes encapsulated as a core protected by the cross-linked hydrophilic corona, since polysilanes exhibit unique electronic spectra depending upon their conformation, which is sensitive to the environment around the chain. SCM-**5e** shows absorption maximum at 333 nm, which is almost identical to those observed for **5e** both in the solid state and in micelle, where the PMHS block takes the trans conformation. This indicates that the PMHS blocks form the unsolvated micelle core, with the cross-linked PMMA forming the solvated corona. In a water-THF mixed solvent, however, the absorption maximum of SCM-**5e** undergoes an abrupt shift from 333 to 305 nm. In THF, SCM-**5e** shows the absorption maximum at 305 nm, indicating that the PMHS block takes a random-coil conformation in THF. The (uncross-linked) block copolymer **5e** in THF also shows absorption maximum at 305 nm.

Nanometer-sized hollow particles. Since the polysilane core part of **5e** can undergo photo-

chemical degradation,[14] it is expected to provide hollow sphere particles (hollow shell cross-linked micelles, HSCM) by a photochemical process as shown in Fig. 13.[15]

Poly(1,1-dimethyl-2,2-dihexyldisilene)-b-poly(methacrylic acid) (**5e**) with a composition of PMHS to PMAA of 1/10 ($Mn = 9.6 \times 10^3$, Mw/Mn = 1.3) was self-assembled in water to form polymer micelles. The formation of near-monodisperse micelles, with an intensity-averaged micelle diameter of 170 nm in water (0.2 g/l, 25 °C), was demonstrated by dynamic light scattering (DLS) studies. Then the carboxylic acid on the poly(methacrylic acid) segment of the block copolymer was subjected to the shell cross-linking reactions with 1,10-diaza-4,7-dioxadecane and 1-ethyl-3-(3-dimethylaminopropyl) carbodiimide hydrochloride similarly as described in the previous section.

The polysilane core part within the shell cross-linked micelles was irradiated by a UV lamp (≥280 nm) for photo-degradation (bleaching). Dialysis against water produced nanometer-sized hollow particles. In UV absorption spectra, a continuous
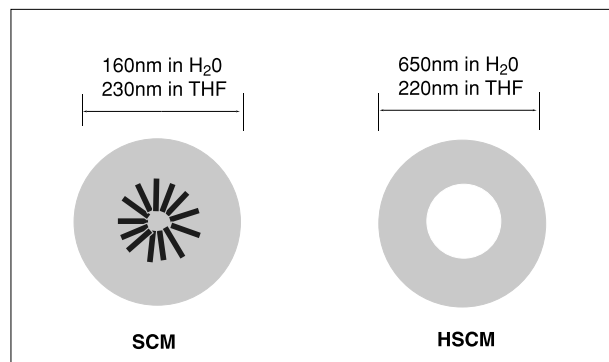
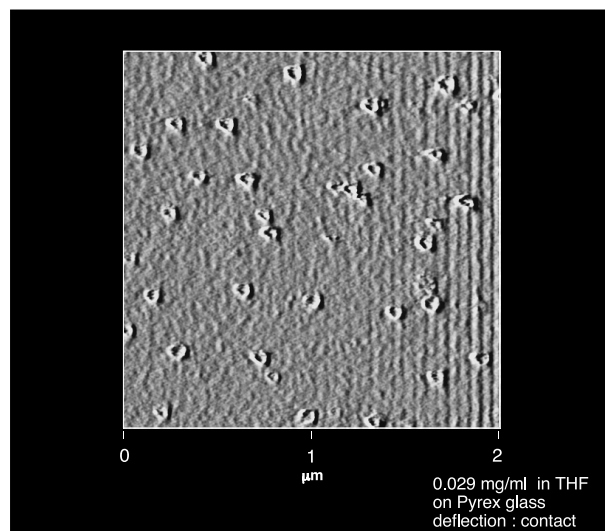Fig. 14. Particle sizes monitored by DLS measurement for SCM-**5**e and HSCM.

Fig. 15. AFM Image of hollow sphere shell cross-linked micelles (HSCM) on Pyrex glass plate with operating in the contact mode.

blue shift in the absorption maximum was observed during photo irradiation, which suggests that the chain scission process of the polysilane core part within the shell cross-linked micelles did occur upon exposure.

Some spectroscopic studies supported the formation of nanometer-sized hollow sphere particles derived from the shell cross-linked micelle templates. Dynamic light scattering (DLS) studies indicated that the average hydrodynamic diameter (D_h) for the hollow particles in water was measured as about 650 nm much larger than the D_h of the template shell cross-linked micelles (160 nm). The significant extent of this expansion can be explained by the swelling of the hydrophilic cross-linked poly(methacrylic acid) layer resulted in removal of the hydrophobic core. However, the diameter of the hollow particle decreased to 220 nm again in THF because of contraction of the cross-linked poly(methacrylic acid) layer under the conditions as shown in Fig. 14.

Images of atomic force microscopy (AFM) gave further information about the size and three-dimensional shapes of the nanometer-sized particles. Fig. 15 shows AFM images of hollow particles on a Pyrex glass plate operating in the contact or tapping mode. Shell cross-linked micelles appeared as clearly spherical particles of about 100 nm diameter in the dry state, indicating that polysilane parts are actually locked into the core. However, after removal of the core within the shell cross-linked micelles, bagel (or liposome)-like objects with diameters of about 100 nm were actually observed. In vertical profiles it appears to be concave shape, although the shells collapsed into a highly flattened form, which agrees well with their hollow-core na-
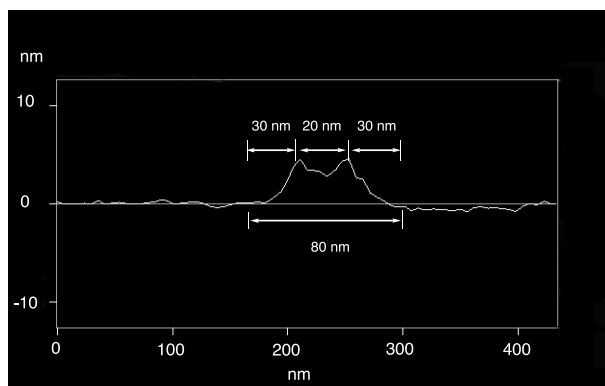

Fig. 16. AFM Image of HSCM; Cross section of the hollow particle shown in Fig. 15.

ture (Fig. 16). The thickness of the shell is consistent with the calculated length of the cross-linked layer (*ca.* 30 nm). The tapping mode AFM images show clearly hollow nanospheres with diameters of about 200 nm when under the wet conditions, because the particles should be swollen to some extent under the conditions.

Functions and some applications of SCM and HSCM. The present system is expected to undergo encapsulation of guest molecules into the core, since the cross-linked corona of both SCM and HSCM may be permeable for small molecules. First, we have examined tetracyanoethylene (TCNE) as a guest molecule. Incidentally, the author reported charge-transfer interactions between polysilanes and
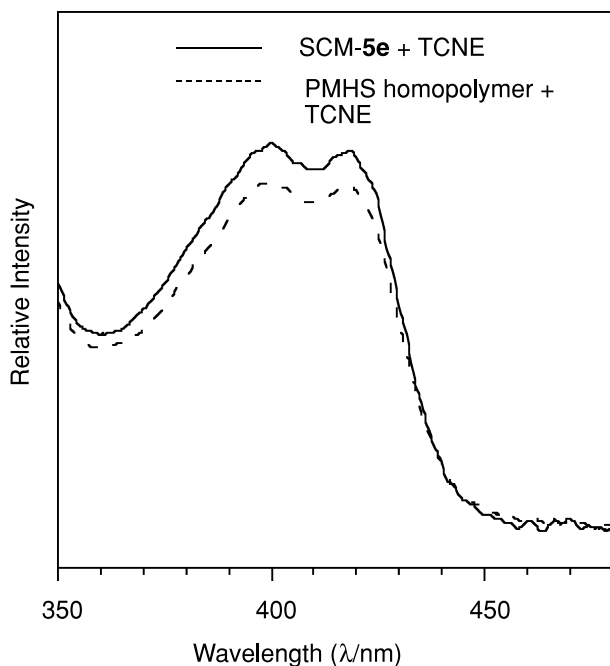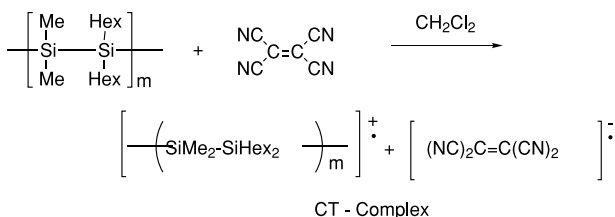
Fig. 17.   UV Spectra of charge-transfer complexes of polysilane and shell cross-linked micelles with TCNE in CH_2Cl_2.

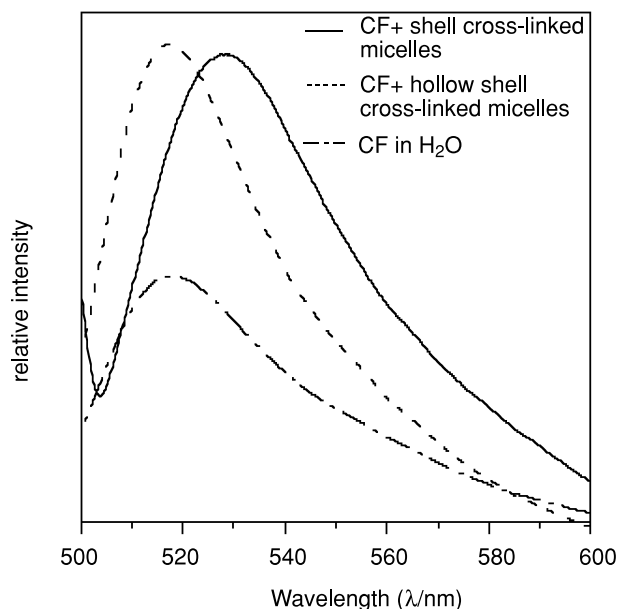
Fig. 18.   Fluorescence emission spectra of 5(6)-carboxyfluorescein (exited at 492 nm) in HSCM and SCM-**5e** in water.

TCNE in 1973.[16] Subsequent studies indicated that this was the first demonstration of charge-transfer interactions between σ- and π- electron systems.[17]

TCNE was added to methylene chloride solutions of both SCM-**5e** and PMHS. The molecular weight of the latter was adjusted same as the polysilane part of SCM-**5e**. Fig. 17 shows UV spectra of charge-transfer complexes of both SCM-**5e** and PMHS. Clearly, identical spectra were observed, indicating that PMHS of the SCM-**5e** interacted with TCNE after encapsulation.

$$[1]$$

Next, encapsulation of 5(6)-carboxyfluorescein (CF) into both shell cross-linked micelles (SCM-**5e**) and nanometer-sized hollow particles (HSCM) was examined. Fig. 18 shows the results. The emission maximum of the entrapped dye into the SCM-**5e** is observed at 528 nm. Contrary, a significant shift in absorption maximum is observed for the dye in

HSCM at 518 nm, the same wavelength as that of the free dye in aqueous solution. This suggests that the dye in HSCM exists in an internal aqueous volume rather than in the hydrophobic domains. After dialysis against water the absorption at 518 nm disappeared gradually, indicating slow release of the dye from a HSCM cage. Preliminary experiments indicated that the release rate was closely related to the degree of cross-linking. This would be important for the future application of these organized systems for drug delivery and similar other uses.

Metal nanoparticles derived from polysilane SCM templates. As described in the previous section, the author has succeeded in synthesizing polysilane SCM, where the polysilane core is surrounded by a partially cross-linked shell of poly(methacrylic acid). By the way, a new method has been reported recently for the synthetic approach to polymeric micrometer- and nanometer-sized particles by cross-linking of the shell of polymer micelles (SCM). Studies on metal particles with nanometer-sized dimensions have also attracted great interest in the diverse fields of materials science because of the unique characteristics resulting from their size. Synthetic approaches using a template strategy have been employed for the preparation of the metal particles. For example, a method has been reported in
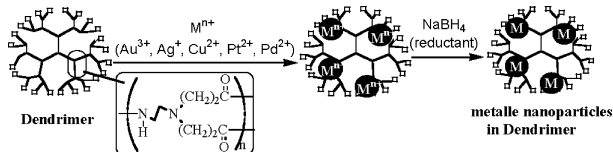
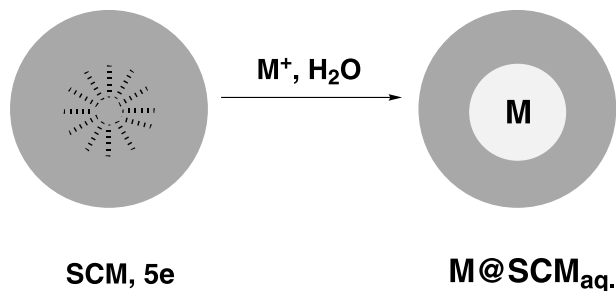Fig. 19.   Reduction of metal ions in SCM.

SCM, 5e   **M@SCM$_{aq.}$**

Fig. 20.   Synthesis of metal nanoparticles (M@SCM) in Water.

Table II.   Oxidation potentials of polysilanes, $(\mathbf{R^1R^2Si})_n$

R^1	R^2	Oxidation Potential/V
methyl	phenyl	0.78
methyl	propyl	0.82
methyl	hexyl	0.95
butyl	hexyl	1.00
hexyl	hexyl	1.00

Diaz, A. F., Baier, M., Wallaff, G. M., Miller, R. D., Nelson, J., and Pietro, W. (1991) J. Electrochem. Soc. **138**, 742.

Table III.   Reduction potentials of some metal ions

$\mathbf{Au^{3+}}$	$\longrightarrow$	**Au :**	E = 1.50 V
$\mathbf{Pd^{2+}}$	$\longrightarrow$	**Pd :**	E = 0.99 V
$\mathbf{Ag^+}$	$\longrightarrow$	**Ag :**	E = 0.88 V
$\mathbf{Cu^{2+}}$	$\longrightarrow$	**Cu :**	E = 0.34 V
$\mathbf{Fe^{2+}}$	$\longrightarrow$	**Fe :**	E = −0.44 V

which metal nanoparticles were prepared by the reduction of metal ions on dendrimers, polymers, and DNA templates with $NaBH_4$, where the template acts to stabilize the metal particles. An example using dendrimers is shown in Fig. 19.[18] Examples of metal nanoparticles with in situ reduction of metal ions on reductive polymers have also been reported. Consequently, new architectures with nanometer-size templates for the synthesis of nanoparticles are being developed.

As described before, polysilane existent in the core of SCM can donate electrons to TCNE to give a charge-transfer complex (eq. [1]). Next, we have applied the ability of reduction of polysilane SCM to the template for the synthesis of metal nanoparticles (M@SCM), as illustrated schematically in Fig. 20.[19] Having relatively low oxidation potentials (Table II), polysilanes are expected to be able to reduce some metal ions (Table III), where the Si-Si bonds undergo oxidation to Si-O bonds.

The requisite polysilane SCM was prepared similarly as shown in Fig. 11 by the shell cross-linking reaction of 2,2'-(ethylenedioxy)bis(ethylamine) and carboxylic acid on the poly(methacrylic acid) segment of the polymer micelles of poly(1,1-dimethyl-2,2-dihexyldisilene)-*b*-poly(methacrylic acid) (Mn = 9.6×10^3, Mw/Mn = 1.3, m/n = l / 12) in water. In a typical preparation of Au nanoparticles using the polysilane SCM template (Au@SCM$_{aq}$), a solution of the SCM (1.8 mg, 2.6×10^{-3} mmol (per Si unit)) and

$HAuCl_4 \cdot 4H_2O$ (2.0 mg, 4.9×10^{-3} mmol) in 10-mL water was stirred for 3 h at room temperature. The reaction mixture gradually changed color from yellow to pinkish-red, indicating the reduction of Au(III) ions to Au(0) particles. A sample of nanoparticles was obtained after dialysis against distilled water. Dynamic light scattering (DLS) studies indicated the presence of particles in water solution. The average diameter of the metal encapsulated SCM was about 25 ($\pm$3.8) nm, much smaller than the diameter of the template SCM (170 nm) in water. In this case, the cross-linked layer can act as a stabilizer to protect the metal particles from aggregation and to maintain solubility in water. Indeed, the resulting aqueous solution of Au(0) nanoparticles was extremely stable, with no precipitation for more than a year. The UV-vis spectrum of the Au@SCM$_{aq}$ particles in H_2O showed an absorption band maximum at 540 nm (Fig. 21), which can be explained by the surface plasmon resonance of Au particles 3–20 nm in size.

Transmission electron microscopy (TEM) images show that the gold particles appeared as clearly spherical particles (Fig. 22 a), where the TEM shows only the metal particle within the SCM because of low contrast for the cross-linked layer. The average diameter, which can be determined from the histogram of the size distribution from the TEM images, was 12 ($\pm$5.7) nm (Fig. 22 b). Since the calculated

Table IV.   Hydrogenation of alkene in aqueous solution in the presence of Pd@SCM

Run	alkene	Solvent	cat./mol%	time/h	yield[a]/%
1	$CH_2=CHCH_2OH$	CH_3OH/H_2O	1×10^{-3}	3	99
2	$CH_2=CH\ CH_2CH_2OH$	CH_3OH/H_2O	1×10^{-3}	3	0
3	$CH_2=CHCH_2OH$	H_2O (b)	1×10^{-3}	3	91
4	$CH_2=CHCH_2OH$	c	1×10^{-3}	3	91
5	$CH_2=CHCH_2OH$	d	1×10^{-3}	3	91
6	$CH_2=CH(CH_2)_3CH_3$	H_2O	0.5×10^{-3}	24	82

a) Yield of 1-propanol determined by NMR.
b) The first Run of the use of catalyst. c) The 2nd Run. d) The 3rd Run.

Fig. 21.   UV-Vis Spectrum of Au@SCM in water.

Fig. 22.   (a) TEM images and (b) particle size distribution of Au@SCM in water.

size of interiors of the template is about 20 nm, the size of the metal particles is somewhat small. The (uncross-linked) micelles from a self-assembly of the block copolymer could also reduce the [AuCl$_4$]- ion, but the size of the resulting Au particles is much larger (25 nm) in average diameter and is widely distributed (±15 nm).

The reduction of Pd(II) ([PdCl$_4$]$^{2-}$) with the polysilane SCM also produced Pd(0) particles (Pd@SCM$_{aq}$) which were highly dispersed in water. The particles were 20 (±10.7) nm in average diameter, as measured on the TEM images. Interestingly, the SCM-stabilized Pd nanoparticles can be used as catalysts for the hydrogenation reaction of alkenes in aqueous solution.
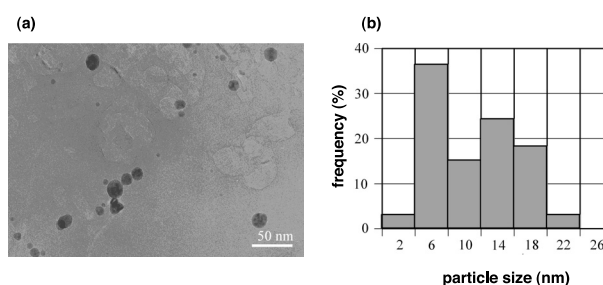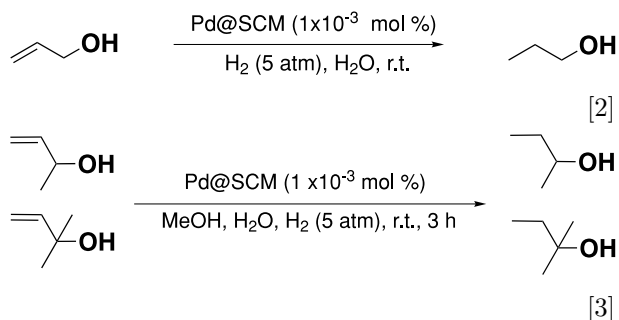
The catalytic hydrogenation of allyl alcohol in aqueous solution under a pressure of 5 atm with the Pd@SCM$_{aq}$ (1×10^{-3} mol%) proceeded smoothly (Table IV). After 3 h, allyl alcohol was converted to give 1-propanol with $> 99\%$ conversion and the turnover frequency (TOF, calculated on the basis of H$_2$ uptake) of 5000 h^{-1} (Run 1).
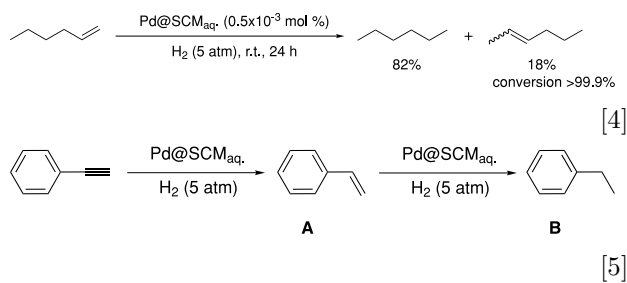

The SCM-Pd nanoparticles were able to hydrogenate 1-hexene and phenylacetylene quantitatively under the same conditions. However, the catalytic performance depends on the substrate structure. The hydrogenation of 3-buten-2-ol did not proceed under the conditions (Run 2), although the hy-
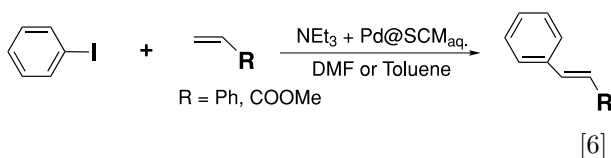
Table V.　Heck reactions catalyzed by Pd@SCM

Ph-I mole ratio	R (of olefin) (mole ratio)	NEt$_3$ mole ratio	solv./ml	time/h	conv./%[a]	yield/%[a]
1	Ph (1.5)	2.1	DMF/1.0	20	89.2	96
1	COOMe (1.7)	2.1	DMF/1.0	20	> 99	82

a) Determined by GC.

drogenation using Pd/C catalyst proceeded (TOF = 7780 and 2300 h^{-1} respectively). Most importantly, the catalyst required no activation, and could be recycled without a decrease in activity (Runs 4 and 5). The catalyst could be recovered after dialysis against water.

[4]

[5]

The Pd@SCM$_{aq}$ could also be employed as catalysts for the Heck reaction of styrene or methyl acrylate with iodobenzene (eq. [6]).

[6]

Although the results are still preliminary, the use of metal nano-particles in aqueous media as catalysts is interesting and promising in future applications.

References

1) (a) West, R. (1986) J. Organomet. Chem. **300**, 327–346. (b) Miller, R. D., and Michl, J. (1989) Chem. Rev. **89**, 1359–1410. (c) Sakurai, H. (ed.) (1996) Advanced Technology of Organosilicon Polymers. CMC Co. Ltd., Tokyo.

2) Sakamoto, K., Obata, K., Hirata, H., Nakajima, M., and Sakurai, H. (1989) J. Am. Chem. Soc. **111**, 7641–7643.

3) Sakamoto, K., Yoshida, M., and Sakurai, H. (1990) Macromolecules **23**, 4494–4496.

4) Sakamoto, K., Yoshida, M., and Sakurai, H. (1994) Macromolecules **27**, 881–882.

5) Sakurai, H., Sakamoto, K., Funada, Y., and Yoshida, M. (1994) *In* Inorganic and Organometallic Polymers II, Advanced Materials and Intermediates, ACS Symposium Series, 572 (eds. Wisian, P., Allcock, V., and Wynne, K. J.). Chapt. 2.

6) Ioka, T. (1995) Ms Theses of Tohoku University.

7) Hirao, A., Kato, H., Yamaguchi, K., and Nakahama, S. (1986) Macromolecules **19**, 1294–1299.

8) Sanji, T., Kitayama, F., and Sakurai, H. (1999) Macromolecules **32**, 5718–5720.

9) (a) Wilhelm, M., Zhao, C. L., Wang, Y., Xu, R., Winnik, M. A., Mura, J. L., Riess, G., and Croucher, M. D. (1991) Macromolecules **24**, 1033–1040. (b) Shikora, A., and Tuzar, Z. (1983) Makromol. Chem. **184**, 2049–2059. (c) Astafieva, I., Zhong, X. F., and Eisenberg, A. (1993) Macromolecules **26**, 7339–7352. (d) Khougaz, K., and Zhong, X. F., and Eisenberg, A. (1996) Macromolecules **29**, 3937–3949.

10) (a) Xu, R., Winnik, M. A., Riess, G., Chu, B., and Croucher, M. D. (1992) Macromolecules **25**, 644–652. (b) Caldérara, F., Hruska, Z., Hurtrez,

G., Riess, G., and Winnik, M. A. (1993) Makromol. Chem. **194**, 1411–1420.

11) (a) Zhang, L., and Eisenberg, A. (1995) Science **268**, 1728–1731. (b) Zhang, L., and Eisenberg, A. (1996) J. Am. Chem. Soc. **118**, 3168–3181. (c) Yu, K., and Eisenberg, A. (1996) Macromolecules **29**, 6359–6361. (d) Yu, Y., and Eisenberg, A. (1997) J. Am. Chem. Soc. **119**, 8383–8384.

12) (a) Thurmond II, K. B., Kowalewski, T., Wooley, K. L. (1996) J. Am. Chem. Soc. **118**, 7239–7240. (b) Thurmond II, K. B., Kowalewski, T., and Wooley, K. L. (1997) J. Am. Chem. Soc. **119**, 6656–6665. (c) Huang, H., Kowalewski, T., Remsen, E. E., Gertzmann, R., and Wooley, K. L. (1997) J. Am. Chem. Soc. **119**, 11653–11659. (d) Wooley, K. L. (1997) Chem. Eur. J. **3**, 1397–1399.

13) Sanji, T., Nakatsuka, Y., Kitayama, F., and Sakurai, H. (1999) Chem. Commun. **21**, 2201–2202.

14) (a) Michl, J., Downing, J. W., Karatsu, T., McKinley, A. J., Poggi, G., Wallraff, G. M., Sooriyakumaran, R., and Miller, R. D. (1988) Pure Appl. Chem. **60**, 959–972. (b) Trefonas, P., West, R., and Miller, R. D. (1985) J. Am. Chem. Soc. **107**, 2737–2742.

15) Sanji, T., Nakatsuka, Y., Ohnishi, S., and Sakurai, H. (2000) Macromolecules **33**, 8524–8526.

16) (a) Sakurai, H., Kira, M., and Uchida, T. (1973) J. Am. Chem. Soc. **95**, 6826–6827. (b) Traven, V. F., and West, R. (1973) J. Am. Chem. Soc. **95**, 6824–6826.

17) (a) Sakurai, H., and Kamiyama, Y. (1974) J. Am. Chem. Soc. **96**, 6192–6194. (b) Sakurai, H. (1980) J. Organomet. Chem. **200**, 261–286.

18) Crooks, R. M., Zhao, M., Sun, L., Chechic, V., and Yeung, L. K. (2001) Acc. Chem. Res. **34**, 181–190.

19) Sanji, T., Ogawa, Y., Nakatsuka, Y., Tanaka, M., and Sakurai, H. (2003) Chem. Lett. **32**, 980–981.

Profile

Hideki Sakurai was born in 1931. He was graduated from the University of Tokyo, Faculty of Science, Department of Chemistry in 1953 and started his research career at the graduate school under the direction of Professor Osamu Simamura in organic free radical chemistry. He received his D. Sc. Degree in chemistry from the University of Tokyo in 1958. After spending a year as Instructor at Osaka City University, he was a postdoctoral fellow at Harvard University with Professor Paul D. Bartlett. He was appointed Associate Professor at Kyoto University in 1963 and started studies on organosilicon chemistry. Unusual physical and chemical behaviors of polysilanes as well as of organosilicon reactive intermediates were disclosed during the five years from 1965, which gave the basis of his systematic studies on organosilicon chemistry. Since 1969 he had been Professor in chemistry at Tohoku University and was Dean of the Faculty of Science (1990-1993). He retired from Tohoku University and moved to Tokyo University of Science in 1995. He served as the president of the Chemical Society of Japan (1996-1997). His research interests include physical organic chemistry, organic synthesis, polymer chemistry, and materials science. His research mainly centers on organosilicon compounds. His pioneering work on allylsilanes as applied to organic synthesis is now known as the Sakurai Reaction. He was awarded Matsunaga Prize (1975), F. S. Kipping Award from the American Chemical Society (1978), the Chemical Society of Japan Award (1981), Wacker Silicone Award (1991), the Imperial Prize and the Japan Academy Prize (1994), the Second Class Order of the Sacred Treasure (2002), and others. He was elected as an honorary member of the Chemical Society of Japan and the Korean Chemical Society.